Cell

Regulation of a Late Phase of T Cell Polarity and Effector Functions by Crtam

Jung-Hua Yeh,[1] Sachdev S. Sidhu,[2] and Andrew C. Chan[1,*]
[1]Department of Immunology
[2]Protein Engineering
Genentech, Inc., 1 DNA Way, South San Francisco, CA 94080, USA
*Correspondence: acc@gene.com
DOI 10.1016/j.cell.2008.01.013

SUMMARY

Spatial organization of cellular proteins plays an important role in establishment of cellular polarity to regulate cell division, differentiation, migration, and organogenesis. Activation of T cells by antigen-presenting cells (APCs) results in the formation of an immunological synapse (IS), assembly of a signaling scaffold at the T cell receptor (TCR) contact, cytoskeletal reorganization, and generation of second messengers within the first hours following intercellular contact. We demonstrate here that Crtam (class-I MHC-*r*estricted *T*-cell *a*ssociated *m*olecule), an immunoglobulin-superfamily transmembrane protein, coordinates a signaling complex anchored by the Scrib polarity protein to establish a later phase of T cell polarity on a subset of CD4⁺ T cells >6 hours following activation. Maintenance of this late cellular polarity results in the ability of CD4⁺Crtam⁺ T cells to selectively produce more IFNγ and IL22. Crtam engagement thus modulates signals many hours beyond the initial activation event and dynamically influences the adaptive immune response.

INTRODUCTION

Coordinate interaction between T cells and APCs is required for efficient TCR activation (Krummel and Macara, 2006). Surface coreceptors, including CD2, CD4, CD8, and CD28, coordinate an initial signaling platform at the T cell:APC contact region to induce changes of membrane dynamics, cell polarity and cell shape required for cytokine production and effector functions. Many TCR-activated genes control subsequent cellular fate and repertoire decisions. Upregulation of transcription factors, such as Tbx21/T-bet, Gata3, Rorc (γt), and Foxp3, regulate T cell subset differentiation (Lee et al., 2006). Upregulation of cell surface proteins, such as CD25, confers IL2 responsiveness and enables cells to undergo cytokine-mediated cell division (Ma et al., 2006). Conversely, upregulation of CTLA4 modulates T cell responses and contributes to shaping the TCR repertoire (Teft et al., 2006). Hence, regulated expression of molecules following TCR activation play important roles in determining T cell responses.

Our search for genes upregulated during T cell activation previously revealed *CRTAM* as a candidate gene upregulated on both human $CD4^+$ and $CD8^+$ T cells (Abbas et al., 2005) (Figure S1A available online). This was consistent with previous reports that human *CRTAM* transcripts are transiently detected in activated $CD8^+$ T cells, NK and NKT cells (Fuchs and Colonna, 2006; Kennedy et al., 2000) and the identification of mouse *Crtam* as an activation-induced gene in thymocytes (Kennedy et al., 2000). Crtam is a type I transmembrane protein containing V and C1-like Ig domains (Du Pasquier, 2004) and contains a highly conserved class I PSD-95/Discs-large/ZO-1 (PDZ)-domain protein-interacting motif capable of assembling large protein complexes involved in a variety of signaling pathways including cellular adhesion, polarity, and proliferation.

In T cells, a network of PDZ-containing proteins, including Scrib and Dlg1, play critical roles in T cell uropod formation, migration, conjugate formation, and T cell functions (Ludford-Menting et al., 2005; Round et al., 2007; Round et al., 2005; Xavier et al., 2004). Mutation of *scribble* (*scrib*) in *Drosophila* or knockdown of Scrib in epithelial cells results in mislocalization of cell junctions, increased cell cycling, and increased cellular proliferation (Bilder et al., 2000; Nagasaka et al., 2006). We report here that Crtam is upregulated on a subset of $CD4^+$ T cells and coordinates a Scrib-centered signaling complex to control a previously unrecognized late phase of T cell polarity and selectively regulates IFNγ and IL22 cytokine production.

RESULTS

Crtam Is Transiently Expressed on a Subset of Activated $CD4^+$ T Cells

Generation of mAbs against mouse Crtam permitted us to confirm that Crtam was not expressed on resting naive $CD4^+CD62L^+$ or $CD8^+$ T cells but was upregulated following TCR activation (Figure 1A and Figure S1B). Expression of surface Crtam was detected in $CD8^+$ T cells within 6 hr following TCR activation and downregulated by 72 hr (Figure S1B). Conversely, Crtam was upregulated on a subset of $CD4^+$ T cells 14 hr following TCR

activation and downregulated within 24 hr (Figure 1A, ~10%–40% of naive and ~5%–15% of effector/memory T cells depending upon the mode of activation; Figure S1B). Upregulation of Crtam in activated naive T cells was further confirmed on FACS sorted $CD44^{lo}CD62L^{+}CD4^{+}$ T cells, *DO11.10 TCR*$^{+}$ *Rag2*$^{-/-}$ $CD4^{+}$ T cells as well as *OT-II TCR*$^{+}$ $CD4^{+}$ thymocytes (Figure S2). The kinetics of Crtam expression on *OT-II TCR*$^{+}$ $CD4^{+}$ T cells in response to OVA/APC stimulation peaked later at 24 hr as compared to anti-CD3/28 mAbs, but was similarly upregulated on a subpopulation of $CD4^{+}$ T cells (data not shown). The inability of Crtam to be upregulated in $CD4^{+}$ T cells was not due to the lack of TCR activation as both $Crtam^{+}$ and $Crtam^{-}$ T cells expressed the CD69 activation antigen (Figure S2C and data not shown).

Several lines of evidence suggested that the presence or absence of Crtam marked two distinct cellular populations. First, Crtam was uniformly upregulated upon TCR restimulation of sorted $CD4^{+}Crtam^{hi}$ (gated ~10%–20% of highest Crtam expressing cells), but not $CD4^{+}Crtam^{-}$ T cells (Figure 1B). Second, GeneCHIP and quantitative TaqMan analysis of sorted 14 hr-activated $Crtam^{+}$ $CD4^{+}$ T cells revealed elevated levels of IFNγ and IL22 mRNAs as compared to $Crtam^{-}$ $CD4^{+}$ T cells (Figure 1C left and data not shown). In contrast, levels of IL2, IL4 and IL13 mRNAs were comparable. Third, restimulation of sorted $Crtam^{+}$ or $Crtam^{-}$ $CD4^{+}$ T cells revealed that $Crtam^{+}$ T cells secreted more IFNγ and IL22, but not IL2 protein than restimulated $Crtam^{-}$ T cells (Figure 1C, right). Analysis of sorted naive $CD4^{+}CD44^{lo}CD62L^{+}$ $Crtam^{+}$ T cells from C57BL/6 or *DO11.10 TCR*$^{+}$ *Rag2*$^{-/-}$ mice revealed a similar preferential secretion of IFNγ and IL22, but not IL2, when compared with $Crtam^{-}$ T cells upon TCR activation (Figures 1D and 1E).

As IFNγ and IL22 are associated with T_H1 and T_H17 cell functions, we further analyzed whether $Crtam^{+}$ and $Crtam^{-}$ cells differed under T_H differentiating conditions. Differentiation of $CD4^{+}$ T cells under T_H1 conditions revealed that $Crtam^{+}$ T cells secreted and produced more intracellular IFNγ (Figures 1F and 1G). Similarly, $Crtam^{+}$ T cells made substantially more IL22 and IL17 when differentiated under T_H17 conditions (Figure 1H). In contrast, no difference in IL4 was detected between $Crtam^{+}$ and $Crtam^{-}$ cells under T_H2 differentiation conditions (Figure 1I). Together, these data suggest that Crtam expression on a subset of naive $CD4^{+}$ T cells is associated with a greater ability to synthesize and secrete IFNγ, IL22, and IL17 cytokines following TCR activation.

Crtam$^{-/-}$ T Cells Have Reduced IFNγ and IL22 Production

To further investigate the physiological function of Crtam, Crtam-deficient mice were generated by homologous recombination (Figure S3A). Gene targeting was confirmed at the DNA and RNA levels (Figures S3B and S3C) and the lack of protein was supported by both flow cytometric and western blot analysis of activated $CD4^{+}$ and $CD8^{+}$ T cells (Figures 2A and 2B). *Crtam*$^{-/-}$ mice were born at expected Mendelian ratios. No thymic developmental defects were detected in *Crtam*$^{-/-}$ mice (Figure S4A) and positive selection of OT-II TCR transgenic thymocytes was normal (Figure S4B). Consistent with the lack of Crtam expression in B lineage cells, no B cell development defects were observed (data not shown). In addition, peripheral B cell numbers and serum immunoglobulin levels were normal (Figure 3F, Figures S4C and S4D, and data not shown). Absolute numbers of immune cells in spleen and blood from *Crtam*$^{-/-}$ mice at 6 weeks of age were comparable to wild-type littermates (Figures S4C and S4D).

Analysis of $CD4^{+}$ *Crtam*$^{-/-}$ T cells under T_H1 differentiating conditions revealed decreased IFNγ mRNA levels, intracellular staining of IFNγ in TCR-activated *Crtam*$^{-/-}$ T_H1 cells (Figures 2C and 2D), and reduced IFNγ secretion following both primary and secondary TCR stimulations when compared to $CD4^{+}$ *Crtam*$^{+/+}$ T cells under T_H1 differentiating conditions (Figure 2E, upper left and Figure S5). Decreases in IL22, and to a lesser degree IL17, were also observed in $CD4^{+}$ *Crtam*$^{-/-}$ T cells under T_H17 commitment conditions (Figure 2E, bottom). A more modest reduction in IL22, but not IL17, was observed when cells were incubated with IL23, a condition that preferentially induces IL22 during primary T cell activation (Liang et al., 2006; Zheng et al., 2007) (Figure S6). In contrast, no difference in IL4 production was observed in *Crtam*$^{-/-}$ T cells differentiated under T_H2 conditions (Figure 2E, upper right). Similar data was generated using $CD4^{+}CD44^{lo}CD62L^{+}$ naive T cells (Figure S7). Hence, loss of Crtam resulted in decreased secretion of IFNγ (a T_H1-associated cytokine) as well as IL22 and IL17 (T_H17-associated cytokines). Similarly, TCR activation resulted in decreased IFNγ secretion in $CD8^{+}$ *Crtam*$^{-/-}$ naive and effector/memory populations (Figure 2F).

As both T_H17 responses and IFNγ are required for host defense against *Citrobacter rodentium*, a noninvasive attaching and effacing bacteria (Mangan et al., 2006), we orally inoculated *Crtam*$^{+/+}$ and *Crtam*$^{-/-}$ mice with C. *rodentium* and analyzed bacterial burden at d7 and 14 postinfection. Consistent with the in vitro defects of *Crtam*$^{-/-}$ T_H1 cells, *Crtam*$^{-/-}$ mice demonstrated > 1 log increase in colonic bacterial burden on d7 and ~2 log increase in splenic pathogen burden at d7 and 14 postinfection (Figure 2G). Together, these data indicate that Crtam deficiency is associated with a selective defect in IFNγ, IL22, and IL17 production and compromised host resistance to oral C. *rodentium* infection.

Crtam$^{-/-}$ T Cells Demonstrate Increased TCR-Mediated Proliferation

In contrast to decreased IFNγ and IL22 secretion, naive $CD4^{+}CD62L^{+}$ *Crtam*$^{-/-}$ T cells expressing an MHC class II-restricted OT-II TCR displayed increased [^{3}H]-thymidine incorporation and increased dilution of CFSE-labeled *Crtam*$^{-/-}$ $CD4^{+}$ T when stimulated with irradiated APCs pulsed with OVA peptides when compared to *Crtam*$^{+/+}$ T cells (Figures 3A and 3B). Similar results were obtained with *OT-I TCR*$^{+}$ $CD8^{+}$ T cells in response to peptide/APC stimulation (Figures 3C and 3D) and when $CD4^{+}$ and $CD8^{+}$ T cells were stimulated with anti-CD3/CD28 mAbs (Figures S8A–S8D). Analysis of $Crtam^{+}$ and $Crtam^{-}$ cells revealed similar results. Sorted $Crtam^{-}$ T cells upon TCR restimulation demonstrated increased [^{3}H]-thymidine incorporation and increased CFSE dilution when compared to sorted $Crtam^{+}$ T cells (Figures S8E and S8F). To ensure that differences in proliferation between $Crtam^{+}$ and $Crtam^{-}$ T cells were not due to extrinsic factors, such as the indirect anti-proliferative effects of IFNγ (Gajewski and Fitch, 1988), CFSE-labeled $CD45.2^{+}$

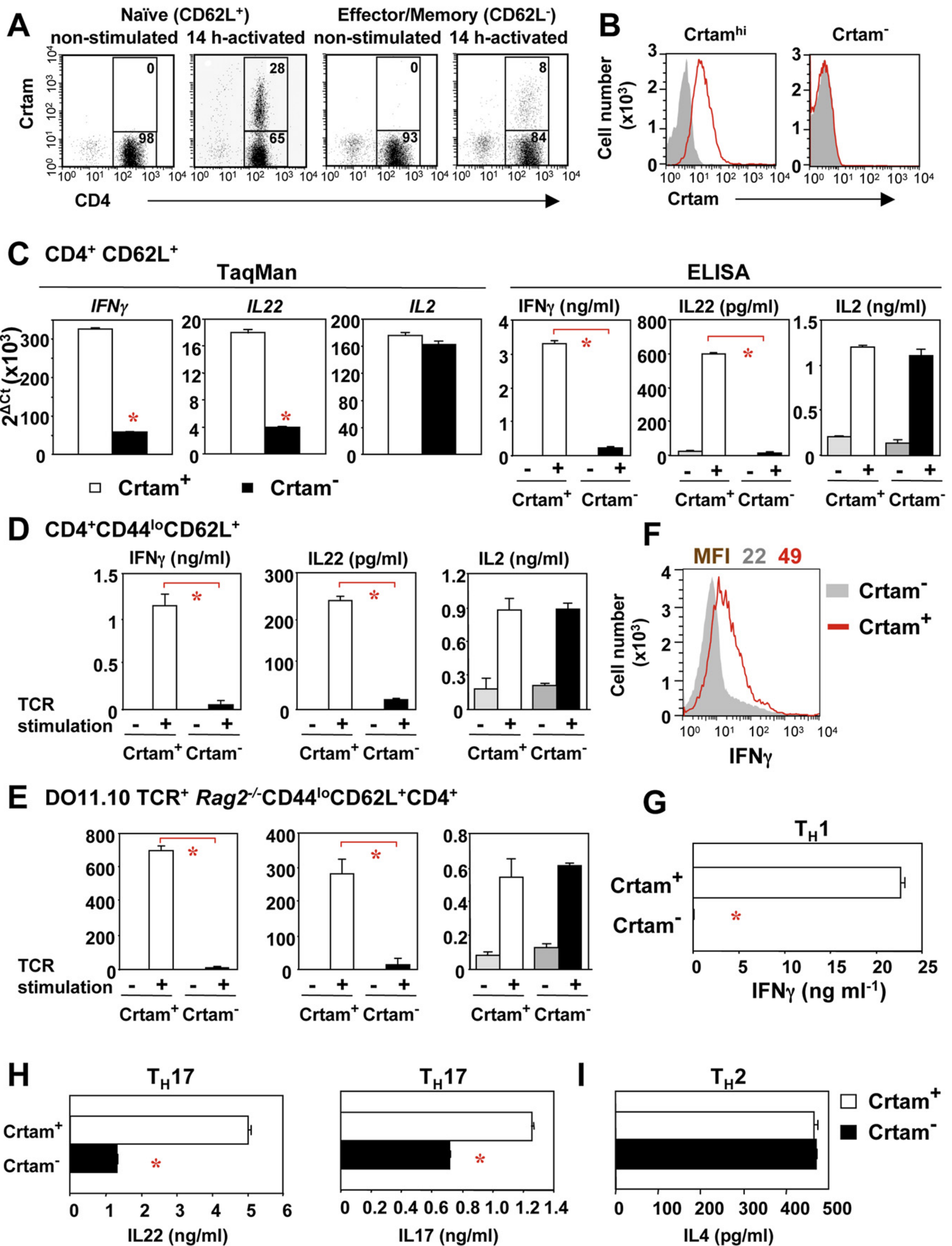
A
Naïve (CD62L+)
Effector/Memory (CD62L-)
non-stimulated
14 h-activated
non-stimulated
14 h-activated
Crtam
CD4
B
Crtamhi
Crtam-
Cell number (x10³)
Crtam
C CD4+ CD62L+
TaqMan
ELISA
IFNγ
IL22
IL2
IFNγ (ng/ml)
IL22 (pg/ml)
IL2 (ng/ml)
2ΔCt (x10³)
Crtam+
Crtam-
D CD4+CD44loCD62L+
TCR stimulation
F
MFI 22 49
IFNγ
E DO11.10 TCR+ Rag2-/-CD44loCD62L+CD4+
G
TH1
IFNγ (ng ml-1)
H
TH17
IL22 (ng/ml)
IL17 (ng/ml)
I
TH2
IL4 (pg/ml)

Crtam$^+$ and CD45.2$^-$ Crtam$^-$ T cells were mixed and activated together with anti-CD3/28 mAbs. Despite coincubation, Crtam$^-$ T cells still proliferated faster and synthesized less IFNγ than Crtam$^+$ T cells (Figures S8F and S8G). Hence, differences in proliferation between Crtam$^+$ and Crtam$^-$ T cells were due to the direct intrinsic function of Crtam.

The in vitro hyperproliferation was also observed in vivo as adoptively transferred CFSE-labeled *Crtam*$^{-/-}$ *OT-II TCR*$^+$ CD4$^+$ T cells demonstrated increased cell divisions in response to OVA immunization when compared to *Crtam*$^{+/+}$ *OT-II TCR*$^+$ CD4$^+$ T cells (Figure 3E). In turn, older *Crtam*$^{-/-}$ mice accumulated CD4$^+$ and CD8$^+$ T, but not B, cells in the peripheral lymph nodes and blood when compared to their wild-type (WT) littermates (Figure 3F). Together, these data indicate that *Crtam*$^{-/-}$ CD4$^+$ and CD8$^+$ T cells demonstrate increased cycling and proliferation in response to TCR activation.

Crtam Assembles a Scrib-Containing Complex that Controls T Cell Polarity 12 hr after TCR Activation

The C terminus of Crtam (ESIV) contains a consensus recognition motif for the PDZ domains of human Scrib ([D/E][T/S]X[LIV]$_{COOH}$) (unpublished data). Hence, we analyzed the ability of Scrib and its related family member, Dlg1, to coimmunoprecipitate with Crtam in resting and activated T cells (Figure 4A). Crtam was detected in Scrib, but not Dlg1, immunoprecipitates 14 hr following TCR activation. This interaction was direct as the third PDZ domain within Scrib was sufficient to bind Crtam (Figure S9A).

The biochemical interaction was further supported by analysis with confocal microscopy demonstrating coaccumulation of Scrib and Crtam in naive T cells activated for 14 hr with plate-bound anti-CD3/28 mAbs (Figure 4B, panels 1–3) and with OVA-pulsed dendritic cells (DCs) (Figure S10A, top). As Scrib and its family members (Dlg1 and Lgl) have been demonstrated to control cellular polarity through Cdc42 GTPase/β-PIX guanine nucleotide exchange factor and Cdc42/Par/PKCζ dependent pathways (Audebert et al., 2004; Osmani et al., 2006), we next analyzed whether the Crtam/Scrib complex controlled Cdc42 and PKCζ localization. In naive CD4$^+$ T cells, TCR activation with plate-bound anti-CD3/28 mAbs or with OVA-pulsed APCs resulted in polarized coaccumulation of Crtam, Scrib, Cdc42, and PKCζ (Figures 4B–4D, panels 1–3; Figures S10A–S10C, top). Conversely, absence of Crtam resulted in loss of Scrib and Cdc42 polarization and coaccumulation (Figures 4B–4D, panels 4–6; Figures S10A–S10C, bottom). Hence, Crtam interacts with Scrib to provide a scaffolding to colocalize Cdc42 and PKCζ containing complexes 12 hr following TCR activation.

To assess the impact of Crtam on localization on other T cell proteins known to polarize upon TCR activation, we stained for CD3, Talin, and CD44 14 hr following TCR activation. Analysis of naive CD4$^+$ T cells revealed that Crtam, Talin, and CD3 coaccumulated at the same region of Crtam$^+$ T cells and were asymmetrically polarized relative to CD44 14 hr following T cell activation with plate-bound anti-CD3/28 mAbs (Figure 4E, panels 4–6; Figure 4F, panels 3 and 4; Figure 4G, panels 7–9). Since T cells lose their tight adhesion to plate-bound anti-CD3/28 mAbs and APCs beginning 6 hr following TCR activation, we were unable to identify the true leading edge of activated T cells 12 hr following TCR activation and refer to the position of the TCR as the TCR/CD3 pole. As the microtubule organizing center (MTOC) as well as the centrosome is reoriented to face the TCR/CD3 pole following receptor activation immediately following TCR engagement (Geiger et al., 1982; Kupfer and Dennert, 1984), we also analyzed MTOC and centrosome positioning relative to the TCR/CD3 pole 12 hr following TCR activation. MTOC and centrosome positioning, visualized by α-tubulin and pericentrin staining, respectively, were both consistently oriented toward CD3 and Crtam 12 hr following activation by plate-bound anti-CD3/28 mAbs (Figure S11). Hence, Talin and Crtam are polarized and CD44 asymmetrically polarized with the TCR/CD3 pole 12 hr following TCR activation.

Asymmetric polarization of CD3/Talin and CD44 was dependent upon Crtam. In *Crtam*$^{-/-}$ T cells, CD3, Talin and CD44 were detected as multiple nonpolarized focal aggregates 14 hr following cocrosslinking of anti-CD3/CD28 mAbs (Figure 4E,

Figure 1. Crtam Is Expressed upon TCR Activation on a Subpopulation of CD4$^+$ T Cells that Produce More IFNγ, IL22 and IL17

(A) Flow cytometric analysis for Crtam expression on splenic CD62L$^+$ and CD62L$^-$ CD4$^+$ T cells 14 hr postactivation with anti-CD3/28(10:2 μg/ml) mAbs. Staining was performed with an anti-Crtam mAb (17B2) and a secondary PE-conjugated anti-hamster Ab (Jackson).

(B) Splenic CD4$^+$CD62L$^+$ T cells from C57BL/6 mice were activated as described above. FACS sorted Crtam^{hi} and Crtam$^-$ T cells were rested 3 days, restimulated at 5×10^5 cells/ml with anti-CD3/28 mAbs, and Crtam expression on restimulated T cells was examined.

(C) Splenic naive CD4$^+$ T cells were activated with anti-CD3/28 mAbs for 14 hr, and mRNA was extracted from sorted Crtam^{hi} and Crtam$^-$ T cells and subjected to quantitative TaqMan analysis (left). Sorted cells were also rested and restimulated as described in (B) and cytokines analyzed at 48 hr (right).

(D) CD44^{lo}CD62L$^+$ CD4$^+$ T cells were purified from C57BL/6 mice by restricted FACS sorting. CD44^{lo}CD62L$^+$ CD4$^+$ T cells (97% purity postsort) were activated with anti-CD3/28 mAbs for 12 hr. FACS-sorted Crtam^{hi} (91% Crtam$^+$ postsort) and Crtam$^-$ (99% Crtam$^-$ postsort) T cells were rested for 3 days, restimulated at 5×10^5 cells/ml with anti-CD3/28 mAbs, and cytokines were analyzed at 48 hr.

(E) CD44^{lo}CD62L$^+$ CD4$^+$ T cells were purified from *DO11.10 TCR*$^+$ *Rag2*$^{-/-}$ mice by FACS sorting (99% purity postsort) and activated with anti-CD3/28 mAbs for 12 hr. Crtam^{hi} and Crtam$^-$ T cells were purified by FACS sorting (both 100% purity postsort), rested 3 days, restimulated at 5×10^5 cells/ml with 0.5 μM OVA pulsed DCs, and cytokines were analyzed at 48 hr. ELISA data shown in (D) and (E) are representative of two independent experiments.

(F) CD4$^+$ T cells were activated under T_H1 condition. 14 hr later, Crtam$^-$ and Crtam^{hi} CD4$^+$ T cells were purified by FACS sorting and thereafter cultured in T_H1 conditional media for 4 days. Differentiated T cells were restimulated with PMA and ionomycin in the presence of GolgiPlug (BD) for 4 hr. Cells were fixed and permeabilized by using BD Cytofix/Cytoperm Plus Kit for immunofluorescent staining of intracellular IFNγ. FACS analysis shown is representative of five (A and B) and three (F) independent experiments. ELISA data shown are representative of five independent experiments (G, H, and I) in which cells were purified from 30 mice.

(G, H, and I) Splenic CD4$^+$CD62L$^+$ T cells from C57BL/6 mice were stimulated with anti-CD3/28 mAbs under T_H differentiating conditions as described in Supplemental Data. 14 hr following TCR activation, FACS-sorted Crtam^{hi} and Crtam$^-$ T cells were rested 3 days, restimulated at 5×10^5 cells/ml with anti-CD3/28 mAbs, and cytokines were analyzed at 48 hr by ELISA.

For all experiments in this manuscript, error bars indicate standard deviation and statistical analysis was performed with a control using Dunnett's Method. * $p < 0.001$.

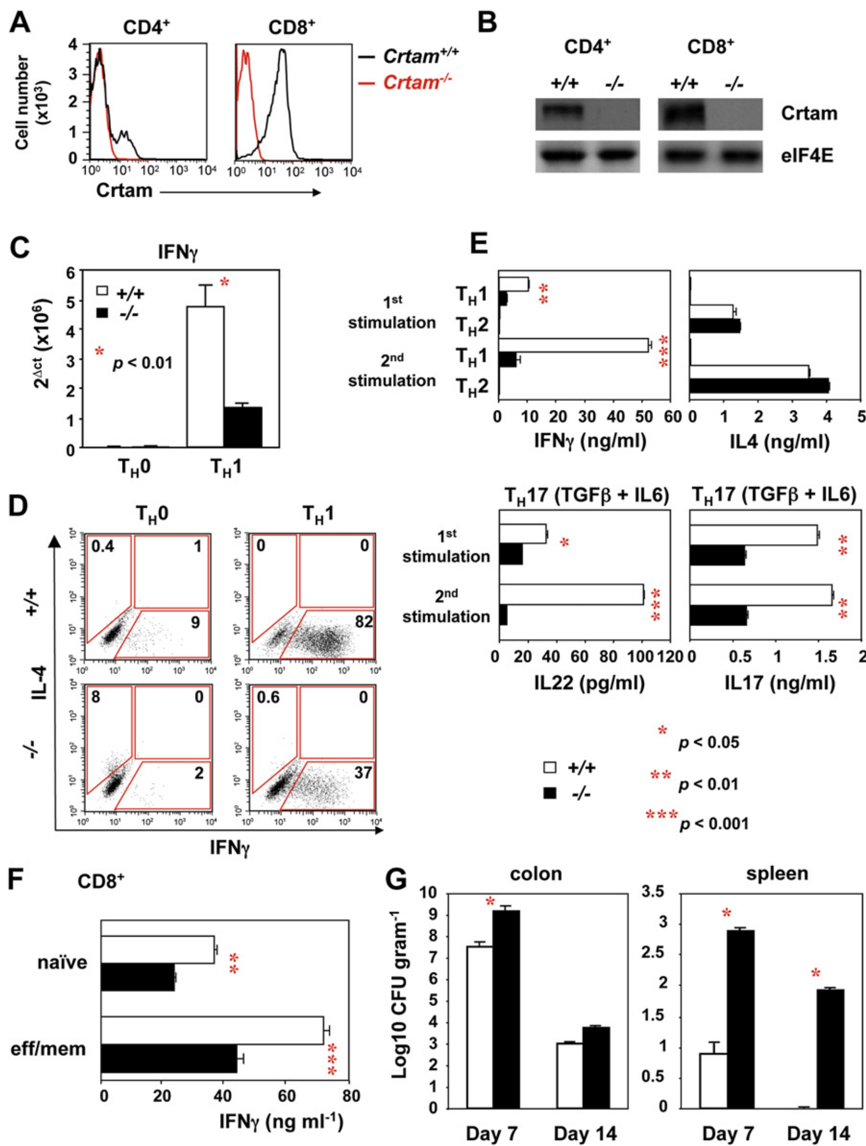

Figure 2. *Crtam*$^{-/-}$ CD4$^+$ and CD8$^+$ T Cells Have Defects in Cytokine Production

(A and B) Crtam expression of 12 hr-activated *Crtam*$^{+/+}$ and *Crtam*$^{-/-}$ T cells was analyzed by flow cytometry (A) and western blot analysis (B).

(C and D) Naive CD4$^+$ T cells were purified from *Crtam*$^{+/+}$ and *Crtam*$^{-/-}$ mice and activated under T_H0 or T_H1 conditions. After 6 days, T cells were washed, reactivated, and cultured in normal media for three additional days. On day 10, differentiated T cells were stimulated with PMA/Ionomycin for 4 hr for TaqMan analysis (C) and PMA/Ionomycin plus GolgiPlug for intracellular staining of IFNγ (D). N = 2 independent experiments.

(E) Naive *Crtam*$^{+/+}$ and *Crtam*$^{-/-}$ CD4$^+$ T cells were activated and cultured in T_H differentiation media. 6 days later, cells were washed, counted, restimulated in normal media at 5 × 10^5 cells/ml with anti-CD3/28(10:2 μg/ml) mAbs, and cytokines were analyzed by ELISA at 48 hr.

(F) Naive (CD8$^+$CD62L$^+$) and effector/memory (CD8$^+$CD62L$^-$) CD8$^+$ T cells were purified and stimulated at 1 × 10^6 cells/ml with anti-CD3/28(10:2 μg/ml) mAbs for naive T cells and 5 × 10^5 cells/ml with anti-CD3/28(5:2 μg/ml) mAbs for effector/memory T cells. Cytokine production was analyzed by ELISA 40 hr following activation. N = 3 independent experiments for (E) and (F).

(G) 10- to 13-week-old mice from an N4 C57/BL-6 Speedy congenic backcross (*Crtam*$^{+/+}$, n = 5; *Crtam*$^{-/-}$, n = 6) were orally inoculated with 2 × 10^9 CFU of *C. rodentium* in 200 μl PBS. Numbers of viable bacteria in the distal colon and spleen were determined on MacConkey agar 7 and 14 days postinfection.

panel 11, Figure 4F, panel 7, and Figure 4G, panel 11). Quantitation of > 200 naive T cells isolated from *Crtam*$^{-/-}$ mice and Crtam$^+$ cells from *Crtam*$^{+/+}$ mice (~40%–50% of all cells from *Crtam*$^{+/+}$ mice are Crtam$^+$ by microscopy) demonstrated the inability of *Crtam*$^{-/-}$ T cells to efficiently polarize Talin, CD44, and CD3 during this latter phase of T cell activation (Figure 4H). Construction of a 3-dimensional model by reconstitution of 2-dimensional slat images further established the focal coaccumulation of Crtam/Talin (Figure S10D, panel 3) and asymmetric polarization of CD44 (panel 4) in *Crtam*$^{+/+}$ T cells as well as the loss of this asymmetric polarity of Talin (panel 5) and CD44 (panel 6) in *Crtam*$^{-/-}$ T cells following TCR activation. Similar defects in Talin, CD44, and CD3 polarization (Figures S10E and S10F) as well as Scrib, PKCζ and Cdc42 colocalization and polarization (Figures S10A–S10C) were observed in naive *OT-II TCR*$^+$ *Crtam*$^{-/-}$ T cells 12–14 hr postactivation using OVA peptide pulsed APCs. Given the lack of CD3 polarization 14 hr following TCR activation, the MTOC as randomly distributed in *Crtam*$^{-/-}$ T cells (Figure S11, bottom).

Much has been learned about the signaling complexes required for establishing cellular polarity within the first minutes to hours following TCR activation (Krummel and Macara, 2006). As Crtam is expressed between 6 to 20 hr following TCR activation and required to maintain polarity of CD3, Talin and CD44 within this timeframe, we hypothesized that distinct molecular complexes may be involved in regulation of the early (0 to 2 hr following TCR activation) and late (8-16 hr following TCR activation) phases of T cell polarity. Hence, we analyzed the localization of CD3, Talin and CD44 and compared the subcellular localization of PKCθ (implicated during the early phase) and PKCζ (implicated in the later phase) using *OT-II TCR*$^+$CD4$^+$ T cells activated with OVA pulsed APCs (Figure 4I and Figure S12). While CD3, Talin and CD44 maintained their polarized localization during the entire 12 hr period following T cell activation (Figure 4I, first three columns), distinct modules of signaling proteins coaccumulated with CD3 during the early (<2 hr) and late (>4 hr) phases following TCR engagement. Consistent with previous reports, PKCθ rapidly colocalized with CD3 (panels 25, 32, and 39) (Monks et al., 1997), but was lost by 4 hr (panel 46) following T cell activation. In comparison, while

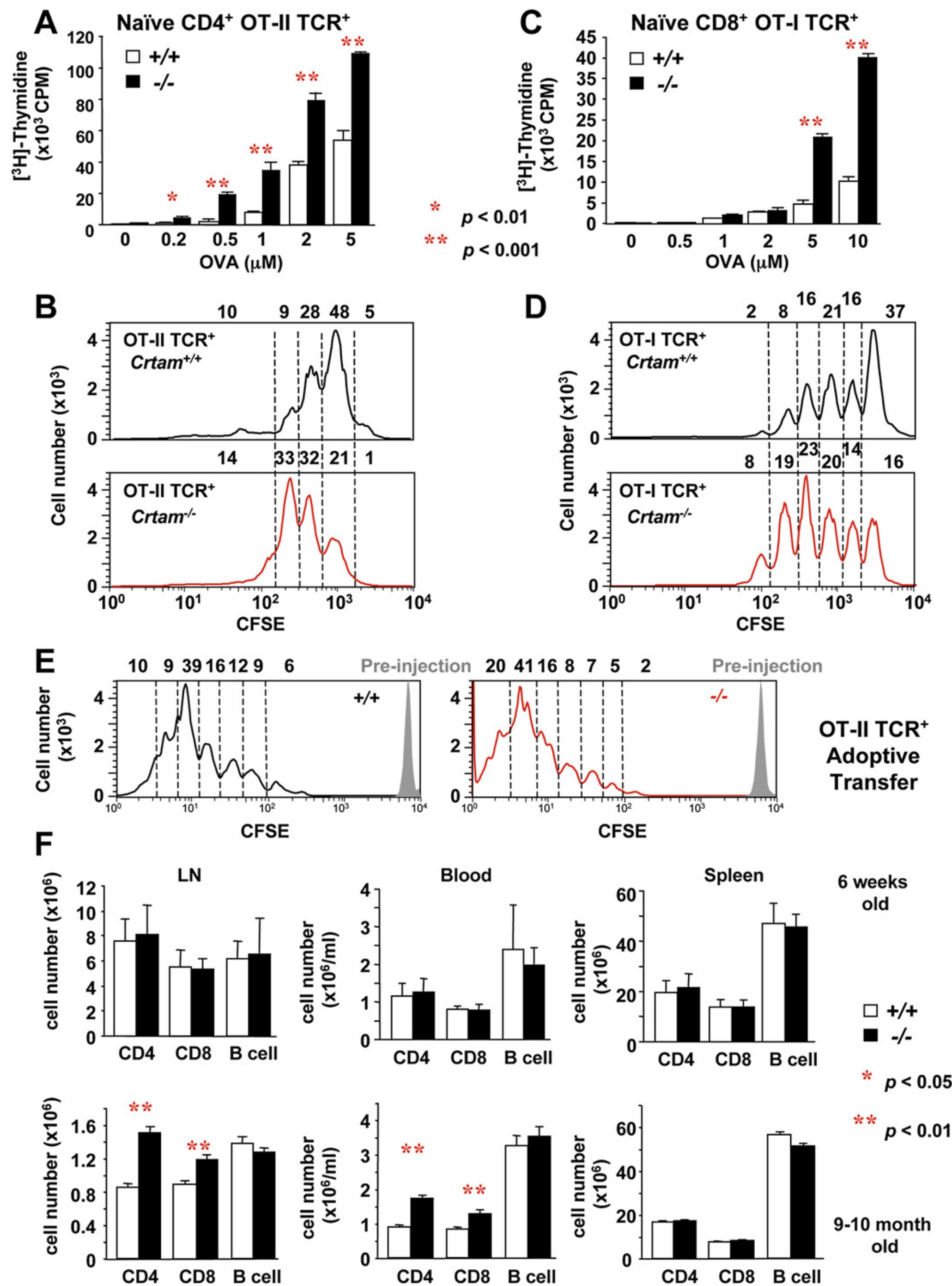

Figure 3. Hyperproliferation of *Crtam*$^{-/-}$ Naive T Cells in Response to APC-Peptide Stimulation

(A–D) Naive *OT-II TCR*$^{+}$ CD4^{+} (A) or *OT-I TCR*$^{+}$ CD8^{+} (C) T cells from *Crtam*$^{+/+}$ and *Crtam*$^{-/-}$ mice were activated with irradiated OVA-loaded APCs, and cellular proliferation was assessed by [^{3}H]-thymidine incorporation. Cell division was monitored by flow cytometric analysis of CFSE-labeled *OT-II TCR*$^{+}$ CD4^{+} (B) or *OT-I TCR*$^{+}$ CD8^{+} T cells (D) activated with 5 and 10 μM OVA, respectively. Percentage of cells within each division are represented above each histogram. Data shown in (A)–(D) are representative of 3 independent experiments.

(E) Enhanced in vivo expansion of *OT-II TCR*$^{+}$ *Crtam*$^{-/-}$ CD4^{+} T cells. CFSE-labeled *OT-II TCR*$^{+}$ CD4^{+} T cells (8 × 10^{6} cells/mouse) from *Crtam*$^{+/+}$ and *Crtam*$^{-/-}$ mice were transferred into B6129SF2/J mice and challenged with 20 μg OVA protein by footpad injection 12 hr following T cell transfer. Draining lymph nodes of recipient mice were analyzed for cell cycling 3 days following antigen challenge. N = 4 independent experiments.

(F) CD4^{+}, CD8^{+}, and B220^{+} cells from cervical lymph nodes (LN), spleen, and blood were quantified from *Crtam*$^{+/+}$ and *Crtam*$^{-/-}$ mice (age 6 weeks, n = 16; age 10 months, n = 10).

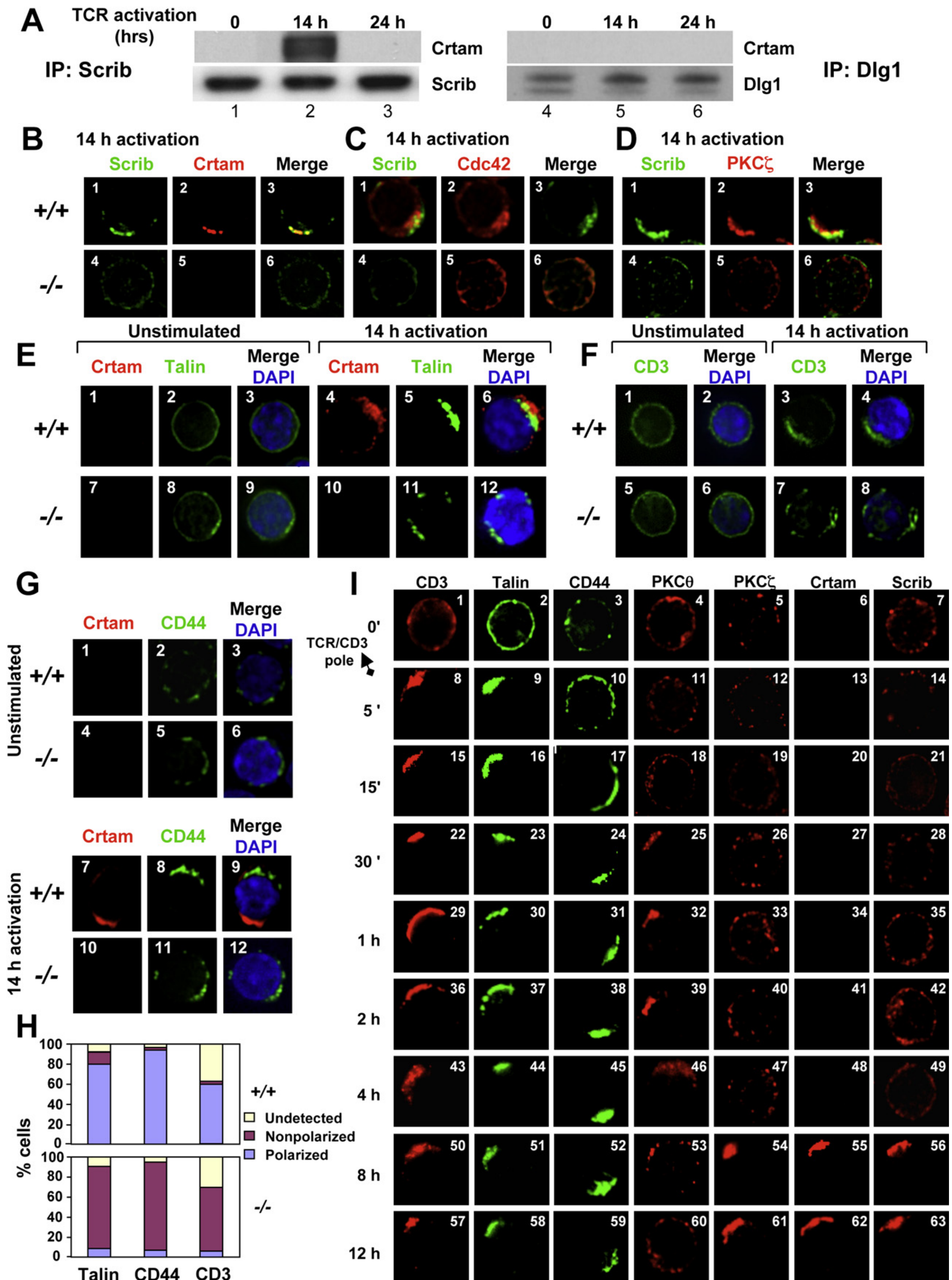
A
TCR activation (hrs)
0
14 h
24 h
IP: Scrib
Crtam
Scrib
1
2
3
0
14 h
24 h
Crtam
Dlg1
IP: Dlg1
4
5
6
B
14 h activation
Scrib
Crtam
Merge
+/+
-/-
C
14 h activation
Scrib
Cdc42
Merge
D
14 h activation
Scrib
PKCζ
Merge
E
Unstimulated
14 h activation
Crtam
Talin
Merge DAPI
F
Unstimulated
14 h activation
CD3
Merge DAPI
G
Crtam
CD44
Merge DAPI
Unstimulated
14 h activation
H
% cells
Undetected
Nonpolarized
Polarized
Talin
CD44
CD3
I
CD3
Talin
CD44
PKCθ
PKCζ
Crtam
Scrib
0'
TCR/CD3 pole
5 '
15'
30 '
1 h
2 h
4 h
8 h
12 h

PKCζ was not colocalized with CD3 within the first 4 hr following T cell activation (panels 12, 19, 26, 33, 40, and 47), the appearance of Crtam resulted in the colocalization of PKCζ with Crtam 8 and 12 hr following T cell activation (panels 54 and 61). Hence, distinct modules of signaling proteins colocalize with CD3 and Talin during the early and later phases of T cell polarity.

While Crtam was required to maintain the later phase of T cell polarity, we also analyzed whether Crtam played any role in the early phase during which it is not expressed. *OT-II TCR*$^{+}$ CD4^{+} *Crtam*$^{-/-}$ T cells activated with OVA pulsed DCs induced polarization of CD3 and Talin to the T cell:APC interface, increased F-actin and localized CD44 to the opposite pole of CD3 within the first 30 min following receptor engagement (Figure S13A). In addition, *Crtam*$^{-/-}$ T cells formed similar numbers of T cell:APC conjugates as assessed by a FACS-based conjugation assay (Figure S13B). As we are unable to predict which 40%–50% of naive T cells from *Crtam*$^{+/+}$ mice would express Crtam 12 hr following TCR crosslinking, we examined the early synapse formation of sorted Crtam^{+} and Crtam^{-} CD4^{+} T cells. Both Crtam^{+} and Crtam^{-} CD4^{+} T cells copolarized CD3 and Talin 30 min following TCR restimulation (Figure S14). Similar to activated naive *Crtam*$^{-/-}$ T cells, defects in Talin polarization were also observed in restimulated Crtam^{-} T cells 14 hr following TCR restimulation (Figure S14B, right). Finally, analysis of TCR-mediated upregulation of CD69 and CD25, increases in free cytoplasmic calcium or induction of tyrosine phosphoproteins on the bulk population did not reveal any differences between Crtam$^{+/+}$ and Crtam$^{-/-}$ T cells (Figures S15A–S15C). Hence, consistent with the lack of Crtam expression on naive CD4^{+} T cells, Crtam does not play any role during the initial phases of T cell:APC conjugate formation, actin polymerization or early TCR-mediated signaling, but is required for establishing T cell polarity during the latter phases of T cell activation.

Requirement for Crtam:Scrib Interaction in Late T Cell Polarity and IFNγ/IL22 Production

To define the structural basis for the requirement of Crtam in Scrib polarization and enhanced cellular proliferation, we utilized retroviral transduction of Crtam, Crtam lacking the entire intracellular domain (ΔICD) or Crtam lacking the C-terminal 4 amino acids required for its interaction with Scrib (ΔESIV) in *Crtam*$^{-/-}$ or *OT-II TCR*$^{+}$ *Crtam*$^{-/-}$ CD4^{+} T cells (Figure 5A). While Crtam reversed the enhanced TCR-mediated proliferation observed with *Crtam*$^{-/-}$ T cells, neither Crtam(ΔICD) nor Crtam(ΔESIV) reversed the hyperproliferative phenotype despite comparable levels of protein reconstitution (Figure 5B, Figures S9B and S16). These data are consistent with the increased cellular proliferation observed with loss of Scrib in *Drosophila* and epithelial cells (Bilder et al., 2000; Nagasaka et al., 2006). Similar to the proliferative phenotype, only full length Crtam restored IFNγ production, IL22 production and Talin polarization (Figures 5C and 5D). Neither Crtam(ΔICD) nor Crtam(ΔESIV) restored the cytokine defects or Talin polarization. Additionally, expression of Crtam, Crtam(ΔICD) or Crtam(ΔESIV) had no effect on TCR-mediated IL2 production. Thus, upregulation of Crtam following T cell activation regulates T cell polarity through its interaction with Scrib that, in turn, controls cellular proliferation and selective cytokine production.

To determine whether expression of Crtam alone was sufficient for IFNγ and IL22 secretion, we sorted naive CD4^{+}CD62L^{+}Crtam^{-} T cells from WT mice and retrovirally transduced Crtam, Crtam(ΔESIV), or a control vector. Expression of WT Crtam in sorted Crtam^{-} T cells from WT mice was sufficient to confer TCR-mediated IFNγ and IL22, but not IL2, production to levels comparable found in sorted TCR-activated Crtam^{+} T cells (Figure 5E). This gain of function was dependent upon the ability of Crtam to interact with Scrib, as Crtam(ΔESIV) was unable to confer TCR-mediated IFNγ or IL22 production. Coincident with gain of TCR-mediated IFNγ and IL22 production, expression of WT Crtam in sorted Crtam^{-} T cells also resulted in Talin polarization (Figure 5F, panel 3), an effect that also required its interaction with Scrib (panel 4). Hence, expression of Crtam can induce Crtam^{-} T cells, isolated from WT mice, to control cellular proliferation, establish cellular polarity and specifically induce IFNγ and IL22 production.

To establish the importance of Scrib in Crtam function, we introduced Scrib siRNA into FACS sorted Crtam^{+} CD4^{+} T cells from C57/BL6 mice. Decrease in Scrib protein was confirmed by western blotting (Figure 6A). Knockdown of Scrib protein resulted in loss of Talin and Crtam polarization 8 hr following anti-CD3/28 mAb crosslinking (Figure 6B) as well as inhibition of TCR-mediated IFNγ and IL22, but not IL2, production (Figure 6C). Scrib expression, however, was not required for the early phase of T cell polarity as measured by staining with anti-CD3,

Figure 4. Crtam Controls Cell Polarity through PDZ Protein Networks

(A) Naive CD4^{+} T cells from *Crtam*$^{+/+}$ mice were activated with anti-CD3/28(10:2 μg/ml) mAbs for the indicated times, and cell extracts were immunoprecipitated with Abs against Scrib (K-21, SCB, left) or Dlg1 (H-60, SCB, right). Immune complexes were analyzed by immunoblotting against Crtam (6E2, GNE), Scrib (H-300, SCB), or Dlg1. N = 5 independent experiments.

(B–D) Naive CD4^{+} T cells were activated with anti-CD3/28(10:2 μg/ml) mAbs for 14 hr. Since T cells activated for > 6 hr lose their tight adhesion with their substrates, T cells were eluted from the plates by gentle pipeting of media. Eluted cells were adhered onto Poly-D-Lysine-coated coverslips (BD BioCoat) for 10–20 min at RT, nonadherent cells were washed off with PBS, and adherent T cells fixed with 4% paraformaldehyde. After fixation, cells were washed again with PBS and stained for Crtam. After the final wash in the surface Crtam-staining protocol, cells were permeabilized with 0.2% Triton X-100 and stained for Scrib, Cdc42, or PKCζ and analyzed by deconvolution microscopy. Images are representative of >300 cells for each staining.

(E–G) Naive *Crtam*$^{+/+}$ (top) or *Crtam*$^{-/-}$ (bottom) CD4^{+} T cells, either unstimulated or stimulated with plate-bound anti-CD3/28(10:2 μg/ml) mAbs for 14 hr, were stained for Crtam and Talin (E), CD3 (F), or Crtam and CD44 (G) and analyzed by deconvolution microscopy.

(H) Polarization of Talin, CD44, and CD3 in *Crtam*$^{-/-}$ T cells and in Crtam^{+} cells of *Crtam*$^{+/+}$ CD4^{+} T cells were quantified by cell counting (n > 200) using deconvolution microscopy (DeltaVision). Note that only ∼40%–50% of all *Crtam*$^{+/+}$ T cells are Crtam^{+} at this time.

(I) Naive *OT-II TCR*$^{+}$ CD4^{+} T cells were activated with OVA-pulsed DCs at 37°C, fixed at defined time points with paraformaldehyde at 4% final concentration, adhered onto 0.01% poly-L-Lysine (Sigma) coated 8-well chamber slides for 20–30 min, nonadherent cells were washed off with PBS, and adherent cells were stained with specific antibodies as indicated above each panel. Surface staining for CD3, CD44, and Crtam was performed before cells were permeabilized with 0.2% Triton X-100. Images are representative of >50 cells for each staining at each time point.

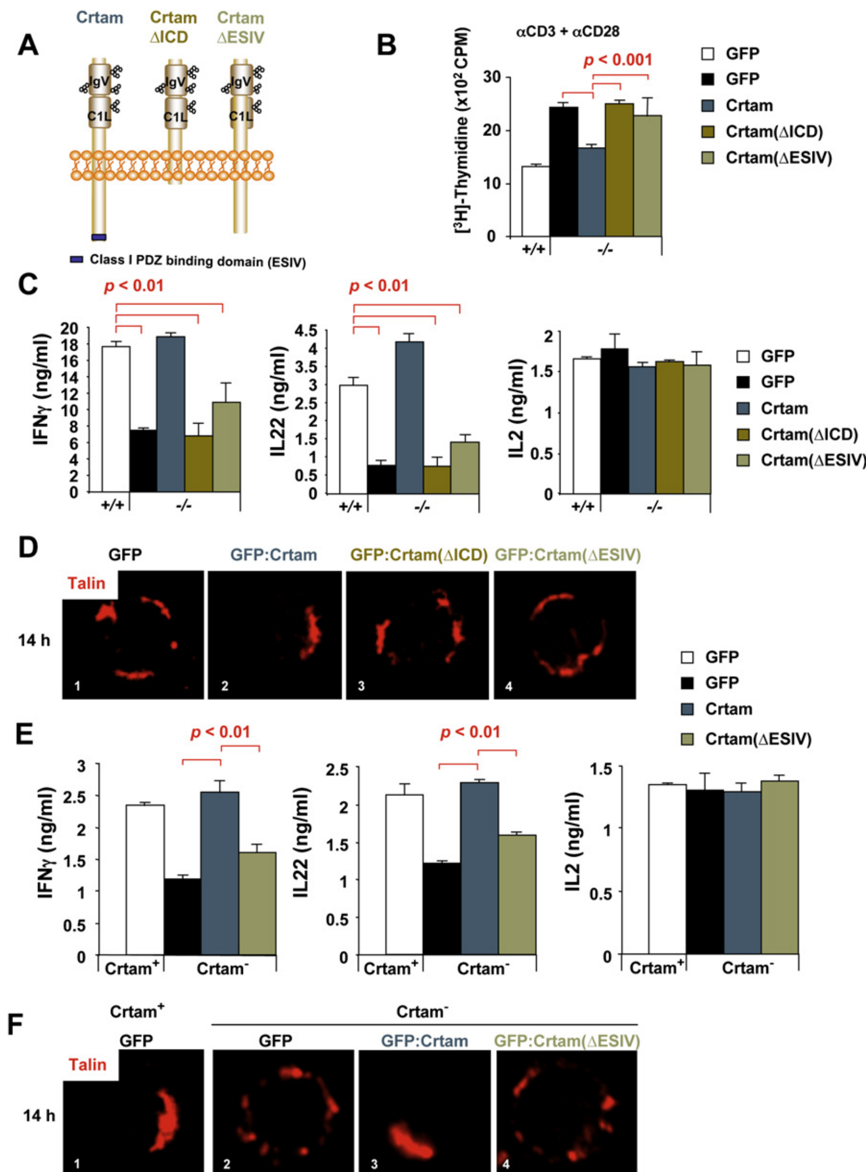

Figure 5. Interaction of Crtam with Scrib Is Requisite to Control Cell Polarity, Proliferation, and Cytokine Production

(A) Structure of Crtam and Crtam mutants.

(B and C) Cellular proliferation and cytokine production of retroviral reconstituted Crtam, Crtam(ΔICD), or Crtam(ΔESIV) in *Crtam*$^{-/-}$ CD4$^+$ T cells. T cells reconstituted with GFP served as a control. Basal levels of [^{3}H]-Thymidine incorporation in nonstimulated GFP control transfected *Crtam*$^{+/+}$ and *Crtam*$^{-/-}$ CD4$^+$ T cells were 235 and 274 cpm, respectively. Cytokine production by nonstimulated GFP transfected CD4$^+$ T cells were: IFNγ: 370 pg/ml (*Crtam*$^{+/+}$) versus 269 pg/ml (*Crtam*$^{-/-}$); IL22: 36 pg/ml (*Crtam*$^{+/+}$) versus 48 pg/ml (*Crtam*$^{-/-}$); IL2: 389 pg/ml (*Crtam*$^{+/+}$) versus 425 pg/ml (*Crtam*$^{-/-}$). N = 5 independent experiments.

(D) Polarity of Crtam, Crtam(ΔICD), or Crtam (ΔESIV) reconstituted *Crtam*$^{-/-}$ CD4$^+$ T cells was examined 14 hr after TCR restimulation.

(E and F) FACS-sorted Crtam$^+$ and Crtam$^-$ CD4 T cells from C57BL/6 mice were retrovirally transduced with GFP, Crtam, or Crtam(ΔESIV). All transfected cells were rested 3 days and restimulated at 2 × 10^5 cells/ml with anti-CD3/28 mAbs. Cytokine production was analyzed by ELISA 48 hr following TCR restimulation (E). ELISA data are representative of n = 4 independent experiments. Talin polarity in Crtam$^+$CD4$^+$ T cells (panel 1) or retrovirally reconstituted Crtam$^-$ CD4$^+$ T cells (panels 2–4) were analyzed 14 hr after restimulation with anti-CD3/28 mAbs (F). Images are representative of >100 cells examined for each staining.

Talin or PKCθ mAbs, or phalloidin following TCR activation (Figure S17A). Similarly, TCR-mediated upregulation of Crtam expression and CD69 was also independent of Scrib expression (Figure S17B).

To further underscore the importance of the Crtam-Scrib interaction, we expressed a chimeric receptor, designated as Crtam(ΔICD):Scrib, consisting of the extracellular and transmembrane domains of Crtam lacking its native intracellular domain (ICD), but fused to a cytoplasmic domain consisting of Scrib. Expression of Crtam(ΔICD):Scrib in *Crtam*$^{-/-}$ T cells was confirmed by western blot analysis (Figure 6D) and FACS staining (Figure 6E). Expression of Crtam(ΔICD):Scrib restored TCR-mediated Talin polarization (Figure 6F, panel 4), control of cell proliferation (Figure 6G) and selectively increased IFNγ and IL22, but not IL2, production (Figure 6H). Collectively, these results underscore the importance of the Crtam:Scrib interaction to regulate this late phase of T cell cytoskeletal polarity and selective cytokine production.

Extracellular Domain of Crtam Regulates Cytokine Production

While the interaction of Scrib with the ICD of Crtam was critical for Crtam function, we also assessed the contribution of the extracellular domain (ECD) of Crtam. Crtam binds cell adhesion molecule (Cadm1, also known as Necl2) that, in turn, can bind itself through homotypic interactions and Cadm3/Necl1 through heterotypic interactions (Galibert et al., 2005; Shingai et al., 2003). In contrast to Crtam, Cadm1 was expressed at low levels on resting naive T cells and its expression was further downregulated 14 hr following TCR activation (Figure S18A). Moreover, confocal microscopy revealed that Cadm1 was diffusely distributed on both resting and activated T cells and did not colocalize with either Talin or Crtam 14 hr following TCR activation (Figure 7A). To assess the contribution of the ECD of Crtam, we expressed a Flag-epitope-tagged mutant of Crtam lacking the ECD, but encoding the transmembrane and intracellular domains of Crtam (aa 251–393) (Figure 7B and Figure S18B). Despite lacking its ECD, expression of Crtam(ΔECD) in *Crtam*$^{-/-}$ T cells retained its ability to polarize with CD3, Talin, Scrib, Cdc42 and PKCζ 8 hr following TCR

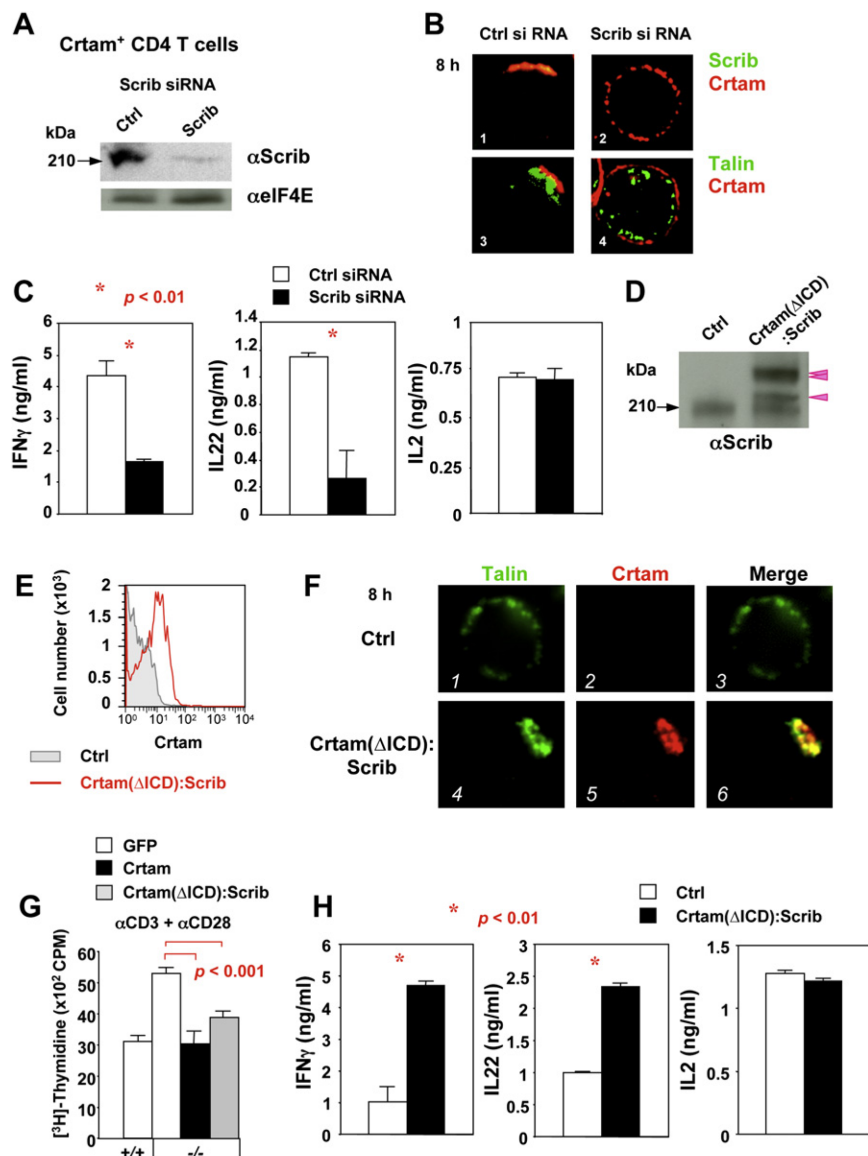

Figure 6. Crtam Function Is Transmitted through Scrib

(A and B) Crtam$^+$ CD4$^+$ T cells from C57/BL6 mice were purified from 14 hr-activated T cells by FACS sorting, expanded 4 days, and electroporated with control or Scrib siRNA (QIAGEN) by Amaxa Nucleofector. 12 hr following transfection, Scrib expression was analyzed by western blotting (A). Arrow indicates endogenous Scrib. T cells were restimulated with anti-CD3/CD28 mAbs for 8 hr and stained for Scrib, Crtam, and Talin (B).

(C) Cytokine production by control or Scrib siRNA transfected cells was analyzed by ELISA 48 hr after restimulation. Cytokine production by nonstimulated siRNA transfected T cells were: IFNγ: 26 pg/ml (control) versus 38 pg/ml (Scrib siRNA); undetectable levels of IL22; IL2: 88 pg/ml (control) versus 103 pg/ml (Scrib siRNA). N = 2 independent experiments.

(D and E) Naive *Crtam*$^{-/-}$ CD4$^+$ T cells were purified and activated with plate-bound anti-CD3/CD28 mAbs. 4 days following stimulation, T cells were electroporated with pIRES-GFP or pIRES-Crtam(ΔICD):Scrib using Amaxa Nucleofector. Expression of Crtam(ΔICD):Scrib was confirmed by western blot analysis(D) and flow cytometry(E). Arrowheads indicate the Crtam(ΔICD):Scrib chimera with its differentially glycosylated forms.

(F) 12 hr following transfection, T cells were restimulated with anti-CD3/CD28 mAbs for 8 hr and cells fixed for staining.

(G) Cellular proliferation of Crtam (ΔICD):Scrib expressing cells was assessed by [^{3}H]-thymidine incorporation. Basal [^{3}H]-Thymidine incorporation in nonstimulated GFP-control transfected T cells was 369 cpm and 426 cpm in Crtam(ΔICD):Scrib transfected CD4$^+$ T cells.

(H) Supernatants of cell cultures were collected 48 hr following TCR stimulation for ELISA analysis. Cytokine production by nonstimulated GFP or Crtam(ΔICD):Scrib transfected T cells were-IFNγ: 52 pg/ml (control) versus 67 pg/ml [Crtam(ΔICD):Scrib]; undetectable levels of IL22; IL2: 76 pg/ml (control) versus 88 pg/ml [Crtam (ΔICD):Scrib]. N = 3 independent experiments.

activation (Figure 7C, panels 6–20). In addition, Crtam(ΔECD) partially reversed the TCR-mediated hyperproliferative phenotype observed in *Crtam*$^{-/-}$ T cells (Figure 7D). Surprisingly, expression of Crtam(ΔECD) was unable to fully restore IFNγ or IL22 production (Figure 7E). Hence, the ECD of Crtam appeared to be dispensable for control of normal cellular division and establishment of a late phase of T cell polarity, but contribute to IFNγ or IL22 production.

To further explore the contributions of the ECD of Crtam in cytokine production, *Crtam*$^{+/+}$ naive T cells were activated with anti-CD3/CD28 mAbs in the absence or presence of a Cadm1 (ECD)-Fc fusion protein encoding the ECD of Cadm1 (aa 1–374) fused to the Fc-domain of human IgG (Figure 7F). Coincubation of Cadm1(ECD)-Fc augmented IFNγ and IL22, but not IL2, production in TCR-activated *Crtam*$^{+/+}$ T cells. In contrast, Cadm1(ECD)-Fc had no effect on cytokine production on *Crtam*$^{-/-}$ T cells. Since expression of Cadm1 and Cadm3 was not affected in *Crtam*$^{-/-}$ T cells (Figure S18A and data not shown), augmentation of IFNγ and IL22 production by Cadm1(ECD)-Fc in *Crtam*$^{+/+}$ T cells is likely to be mediated by Cadm1:Crtam interactions. Collectively, these data distinguish functional contributions by the ligand binding of Cadm1 to the ECD of Crtam in the selective regulation of IFNγ and IL22 production and the contributions of the transmembrane and IC domains of Crtam in establishing cellular polarity and the control of cell division.

DISCUSSION

Reorganization of the T cell cytoskeleton during the first hours following cellular activation is important for establishment of cellular polarity, MTOC reorganization, efficient and sustained generation of second messengers, and subsequent T cell effector functions. While the initial phase of cytoskeletal reorganization

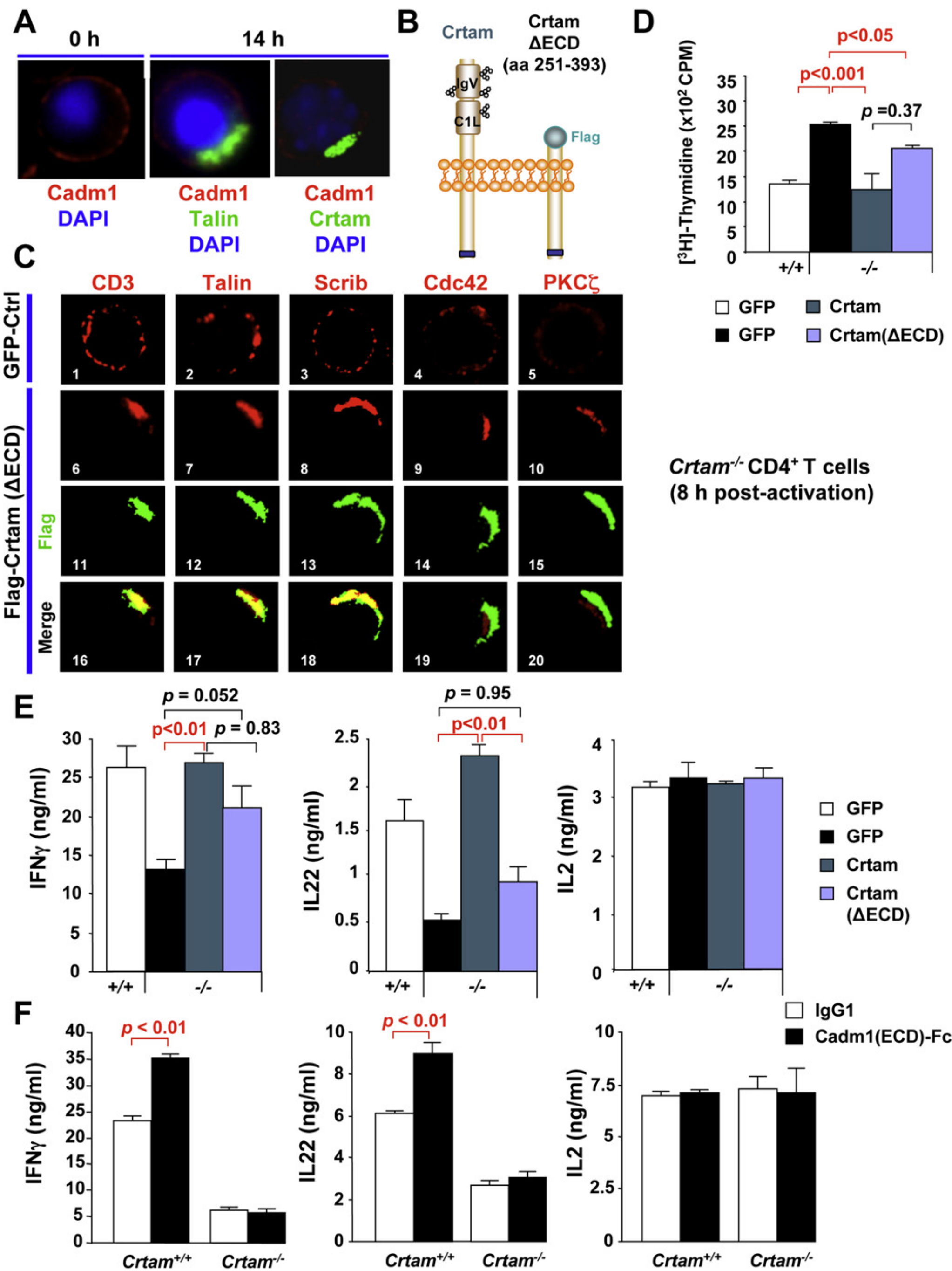

Figure 7. Intracellular Domain of Crtam Controls T Cell Polarity and Proliferation, and the Interaction of Cadm1 and Crtam Can Further Enhance Cytokine Production of CD4 T Cells

(A) Naive CD4$^+$ T cells, either unstimulated or stimulated with anti-CD3/28 (10:2 μg/ml) mAbs for 14 hr, were stained with anti-Cadm1 rabbit polyclonal Ab (GNE) plus Talin or Crtam and analyzed by deconvolution microscopy.

(B) Structure of Crtam and Crtam(ΔECD) mutant.

(C) Naive *Crtam*$^{-/-}$ CD4$^+$ T cells were purified and activated with plate-bound anti-CD3/28 mAbs. 4 days following stimulation, T cells were retroviral reconstituted with GFP or Flag-Crtam(ΔECD). Polarity of GFP or Crtam(ΔECD) reconstituted *Crtam*$^{-/-}$ CD4 T cells was examined at 8 hr after TCR restimulation.

(D) Cellular proliferation of Crtam or Flag-Crtam(ΔECD) transfected *Crtam*$^{-/-}$ CD4$^+$ T cells was assessed by [^{3}H]-thymidine incorporation. *Crtam*$^{+/+}$ and *Crtam*$^{-/-}$ CD4$^+$ T cells transfected with GFP served as controls.

(E) Cytokines were analyzed by ELISA at 48 hr following TCR stimulation.

(F) Naive *Crtam*$^{+/+}$ and Crtam$^{-/-}$ CD4$^+$ T cells were purified, activated with plate-bound mAbs plus plate-bound Cadm1(ECD)-Fc (1 μg/ml) or human IgG1 (1 μg/ml), and cytokines measured at 48 hr. N = 2 independent experiments.

involves recruitment of PKCθ, Vav1/Vav, Was/Wasp, Wasf2/WAVE2, and Hcls1/HS1 to the IS within the first hour of T cell activation (Krummel and Macara, 2006), our studies here reveal an additional latter phase of cellular polarization important in a subset of CD4$^+$ T cells requiring Crtam beginning 6 hr following TCR activation. Crtam binds Scrib via a C-terminal motif that, in turn, organizes a complex involving PKCζ and Cdc42. The Crtam-Scrib interaction is required to assemble this molecular complex and to maintain T cell polarity beyond the early phase of T cell activation. In the absence of Crtam-Scrib interactions, T cells are unable to sustain CD3, Talin, and CD44 polarization and segregation >6 hr following the initiation of T cell activation. Hence, divergent signaling machinery is involved in initiating and maintaining T cell polarity.

The Scrib family of proteins (Scrib, Dlg, and Lgl) serves as scaffolding proteins to control cell polarity and proliferation (Humbert et al., 2006). In *Drosophila* and epithelial cells, loss of these genes results in mislocalization of apical proteins and adherens junctions, enhanced cellular proliferation, reduced differentiation capacity, and lower thresholds to cellular transformation. Control of epithelial polarity and cellular proliferation, through mutational analysis of Scrib, appears to be tightly linked (Zeitler et al., 2004). Our studies demonstrate a similar regulatory pathway for late T cell polarity and control of cellular proliferation. Reconstitution of Crtam$^-$ or *Crtam*$^{-/-}$ T cells with WT Crtam, the Crtam(ΔICD):Scrib chimera, or the Crtam(ΔECD) mutant is sufficient to restore T cell polarity and control cellular proliferation. Scrib interacts with a variety of effector proteins, including the βPIX-GIT guanine nucleotide exchange factor for Cdc42 and Rac GTPases at the leading edge of polarizing astrocytes (Audebert et al., 2004; Osmani et al., 2006). While Scrib and Par complexes are both required for directed migration in *Drosophila* epithelia, they can play both cooperative and antagonistic roles (Humbert et al., 2006). Scrib complexes restrict Par complexes to the apical membrane and Par/Crumbs complexes exclude Scrib complexes to the apical membrane (Bilder et al., 2003; Tanentzapf and Tepass, 2003). Conversely, in migrating astrocytes, activation of Cdc42 controls Par6-PKCζ localization and activation at the leading edge of migrating astrocytes to spatially regulate Dlg1 (Scrib) complexes and the association of adenomatous polyposis coli (APC) with microtubule plus ends (Etienne-Manneville et al., 2005). In addition, Scrib transiently localizes to the leading edge of migrating T cells or at sites of new cell-cell interaction that overlap with aPKC (PKCζ and PKCλ) (Humbert et al., 2006). Hence, the relationship between Scrib and Par-aPKC complexes in T cells during both early and late phases following receptor activation is highly dynamic and requires additional investigation.

Involvement of the Scrib family has been described in a variety of phases of T cell activation. Establishment of T cell polarity has been recently linked during asymmetric T cell division to the generation of disparate memory and effector T cell fates (Chang et al., 2007). In P14 TCR$^+$ CD8$^+$ T cells activated in vivo following infection with Listeria monocytogenes, Scrib polarizes with CD3 while PKCζ polarizes to the opposite pole. In our study, we focused on a much earlier timeframe (~12 hr) following TCR activation of CD4$^+$ T cells when T cells are not preparing for cell division. At 12 hr, we find Crtam polarized with TCR/CD3, Scrib, Cdc42, and PKCζ. Scrib has also been described to be dynamically regulated during the first 30 min following TCR activation (Ludford-Menting et al., 2005). Activation of both CD8$^+$ T cell blasts and the MD45 CD8$^+$ cytotoxic T cell line (CTL) reveals that Scrib is initially recruited to IS of T cells opposite of CD3 (5 min after TCR activation), and then polarized opposite to CD3 and the IS at 15 min. In contrast to Scrib and similar to our findings on the early phase of T cell polarity, PKCζ is not polarized and remains diffusely distributed within the cytoplasm. Knockdown of Scrib using siRNAs in MD45 CD8$^+$ CTLs decreases uropod formation as well as spontaneous IS and T cell:anti-CD3 bead conjugate formation. In our study, we did not observe polarization of Scrib in naive CD4$^+$ T cells up to 4 hr following TCR activation. In addition, knockdown of Scrib in CD4$^+$ T cells did not affect PKCθ or Talin localization with CD3 or upregulation of CD69 and CD25 following TCR activation. Differences observed in Scrib at these early time points may reflect differences in experimental systems. In addition to Scrib, its related family member Dlg1 containing 3 PDZ domains has also been implicated in early TCR-mediated polarization and function. Dlg1 colocalizes with CD3 and cortical actin within 15 min following TCR activation (Round et al., 2005; Xavier et al., 2004). Knockdown of Dlg1 with siRNAs in OT-1 CD8$^+$ T cells results in decreased CD3 clustering, F-actin formation, cytolysis, and cytokine production (Round et al., 2005), though knockdown of Dlg1 in Jurkat T cells enhances NFAT transcription (Xavier et al., 2004). This notwithstanding, these studies indicate that Scrib family of proteins play dynamic roles during distinct stages of T cell activation.

Prolonged maintenance of T cell polarity, through Crtam:Scrib, contributes to IFNγ and IL22 production. Mutation of the Scrib interacting site at the C terminus of Crtam has a selective effect on IFNγ and IL22 production, and to a lesser degree IL17. Sorted Crtam$^-$ T cells or cells expressing Crtam mutants unable to interact with Scrib do not establish late T cell polarity and secrete less IFNγ and IL22 than Crtam$^+$ T cells. This selective effect, at minimum, involves transcriptional activation of these genes as mRNAs of IFNγ and IL22 are augmented in Crtam$^+$ and *Crtam*$^{+/+}$ cells when compared to Crtam$^-$ and *Crtam*$^{-/-}$ T cells, respectively.

In contrast to requirement of the Crtam-Scrib interaction for maintenance of late-phase T cell polarity, control of cellular division, and IFNγ/IL22 production, the ECD of Crtam, while dispensable for polarity and proliferation, contributes to the regulation of IFNγ/IL22 production. Engagement of Crtam's ligand, Cadm1, augments TCR-mediated IFNγ/IL22 production in *Crtam*$^{+/+}$, but not *Crtam*$^{-/-}$, T cells. As Cadm1, the ligand for Crtam, is expressed on a subset of mouse DCs within T cell zones as well as on epithelial cells (Galibert et al., 2005; Shingai et al., 2003), the contributions of Cadm1 binding to Crtam within these microenvironments likely influences the functional programs of Crtam$^+$ T cells. Cadm1 expressing cells augment IL22 mRNA expression of CD8$^+$ T cells and natural killer cell responses (Boles et al., 2005; Galibert et al., 2005). As Crtam preferentially induces IFNγ and IL22, Cadm1:Crtam interactions on CD4$^+$ T cells may influence T_H1 and T_H17 biology.

While our studies do not presently demonstrate a role for Crtam in T lineage commitment, linkage between cytoskeletal reorganization and T cell differentiation has been suggested by several observations. Colocalization of IFNγR with the TCR within the

immunological synapse is associated with T_H1 lineage commitment and is inhibited by T_H2 differentiation (Maldonado et al., 2004). In humans, T cells deficient in the WAS protein not only exhibit defective cytoskeletal reorganization, but also demonstrate selective defects in TCR-mediated IFNγ and IL2, but not IL4, IL5, or IL10, transcriptional activation (Trifari et al., 2006). In addition to subcellular cytoskeletal reorganization, strength and duration of TCR signals can also affect T lineage commitment. T_H1 differentiation can be induced with shorter duration of stimuli or lesser costimulation requirements while IL4 secretion requires longer TCR triggering (Holzer et al., 2003; Iezzi et al., 1999). Others have demonstrated that very low and very high antigen doses favor Th2-like cells (Hosken et al., 1995). Engagement of $Crtam^+$ T cells 14 hr following initiation of TCR activation with specialized cells that express or upregulate Cadm1 may provide an additional level of regulation of T cell differentiation and function.

Unlike other activation markers, such as CD69 and CD25, where the entire population of activated T cells expresses the upregulated marker, only a subset of activated $CD4^+$ T cells express Crtam. The ability of T cells to upregulate Crtam likely reflects a stochastic event following T cell activation. While we cannot presently exclude other peripheral instructional signals that influence Crtam expression on naive $CD4^+$ T cells, Crtam is upregulated on a subset of mature $CD4^+$ thymocytes ex vivo with anti-CD3/28 crosslinking and argues against an instructional model once cells exit the thymus. While the factors that define Crtam expression in activated T cells are presently unknown, Crtam expression imprints a transcriptional program that maintains Crtam expression in its progeny. $Crtam^{hi}$ T cells homogeneously express Crtam upon TCR reactivation. Conversely, $Crtam^-$ cells do not express Crtam upon reactivation. While $Crtam^+$ and $Crtam^-$ effector cells upon reactivation still differ in IFNγ, IL22, and IL17 production, establishment of late T cell polarity and cellular proliferation, these effector cells also differ in their signaling cascades upon TCR activation (unpublished data). Additional studies are ongoing to define how these signaling differences relate to in their different functional outcomes. Together, our data support the idea that Crtam organizes a molecular scaffold through Scrib to regulate a previously unrecognized later phase of T cell activation and demonstrates that signals delivered beyond the first few hours of T cell activation continue to influence epigenetic changes in DNA and chromatin structure to influence T cell functions.

EXPERIMENTAL PROCEDURES

Immunofluorescence Microscopy

For studies on early T cell polarity, DCs were positively purified by CD11c MicroBeads (Miltenyi Biotec) and labeled with 0.5 μM Cell Tracker Orange CMRA (Molecular Probes). After incubation with 5 μM $OVA_{323-339}$ for 1 hr, DCs were incubated with naive $CD4^+$ T cells for 30 min at 37°C, and cells adhered onto Poly-D-Lysine-coated coverslips (BD BioCoat) for 10–20 min at RT before fixation. For FACS sorted *OT-II TCR*$^+$$Crtam^+$ and $Crtam^-$ $CD4^+$ T cells, cells were rested for 3 days before restimulation.

For studies on late T cell polarity, $CD4^+$ T cells were either activated with plate-bound anti-CD3/28 mAbs or OVA/APCs for 12–14 hr at 37°C. Activated T cells were flushed off the plate by gentle pipeting with media. Eluted cells were adhered onto Poly-D-Lysine-coated coverslips (BD BioCoat) for 10–20 min at RT, nonadherent cells were washed off with PBS, cells were fixed with 4% paraformaldehyde in PBS, stained with anti-Crtam hamster polysera or mAb (17B2, Genentech), anti-CD44 mAb or anti-CD3 mAb, permeabilized with 0.2% Triton X-100, and stained with anti-Talin (Sigma), anti-PKCθ (Cell Signaling), phalloidin (Molecular Probes) for F-actin, anti-Scrib (H-300), anti-Cdc42 (B-8), or anti-PKCζ (H-1) antibodies from Santa Cruz Biotechnology (SCB). DAPI-containing mounting medium (Vector Labs) was used to visualize DNA. Slides were analyzed by deconvolution microscopy (Delta Vision). The 3D models of staining were reconstituted using Imaris 5.5.

Constructs, Retroviral Reconstitution, and siRNAs

The Crtam(ΔICD):Scrib chimera was generated by fusing full-length MmScrib cDNA to the C-terminal of Crtam(ΔICD, aa 1–316) using a BamHI site and subcloned into a pIRES2-EGFP vector. siRNAs for Scrib were obtained from QIAGEN and are detailed in Supplemental Data. 4 μg of plasmid DNA or 0.25 μg/siRNA for a total 1 μg mixture of Scrib or control siRNA was used in electroporation with 5×10^6 cells using Mouse T cell Nucleofector kit (Amaxa) and Amaxa Nucleofector (Program X-01). Retroviral expression of WT Crtam, ΔICD(aa 1–316), ΔESIV, or ΔECD(aa 251–393) mutants with a downstream internal ribosomal entry site promoter-driven eGFP was performed as previously described and further detailed in Supplemental Data (Pear et al., 1993).

Abs Used and Proliferation Assays

Abs used for staining were purchased from BD PharMingen unless otherwise specified. Microbead-enriched naive $CD4^+$ or $CD8^+$ T cells (2×10^4) from splenocytes were cultured in flat-bottomed MaxiSorp surface microplates (Nunc) coated with anti-CD3/28 (10:2 μg/ml) mAb or irradiated 5 μM OVA pulsed APCs. After 42 hr, [^{3}H]-thymidine (1 μCi/well) was added, and plates were harvested 8 hr later. For Carboxyfluorescein diacetate-succinimidyl ester (CFSE) labeling, cells were labeled with 5 μM CFSE by CellTrace CFSE Cell Proliferation Kit (Molecular Probes), and proliferating cells were harvested 3 days later for FACScan analysis.

SUPPLEMENTAL DATA

Supplemental Data include Supplemental Experimental Procedures, eighteen figures, and Supplemental Acknowledgments and can be found with this article online at http://www.cell.com/cgi/content/full/132/5/846/DC1/.

ACKNOWLEDGMENTS

A multitude of individuals listed in the Supplemental Data provided invaluable discussion, reagents, and technical contributions. Authors are employees of Genentech, Inc.

Received: July 25, 2007
Revised: October 22, 2007
Accepted: January 8, 2008
Published: March 6, 2008

REFERENCES

Abbas, A.R., Baldwin, D., Ma, Y., Ouyang, W., Gurney, A., Martin, F., Fong, S., van Lookeren Campagne, M., Godowski, P., Williams, P.M., et al. (2005). Immune response in silico (IRIS): immune-specific genes identified from a compendium of microarray expression daSta. Genes Immun. *6*, 319–331.

Audebert, S., Navarro, C., Nourry, C., Chasserot-Golaz, S., Lecine, P., Bellaiche, Y., Dupont, J.L., Premont, R.T., Sempere, C., Strub, J.M., et al. (2004). Mammalian Scrib forms a tight complex with the betaPIX exchange factor. Curr. Biol. *14*, 987–995.

Bilder, D., Li, M., and Perrimon, N. (2000). Cooperative regulation of cell polarity and growth by Drosophila tumor suppressors. Science *289*, 113–116.

Bilder, D., Schober, M., and Perrimon, N. (2003). Integrated activity of PDZ protein complexes regulates epithelial polarity. Nat. Cell Biol. *5*, 53–58.

Boles, K.S., Barchet, W., Diacovo, T., Cella, M., and Colonna, M. (2005). The tumor suppressor TSLC1/NECL-2 triggers NK-cell and CD8+ T-cell responses through the cell-surface receptor CRTAM. Blood *106*, 779–786.

Chang, J.T., Palanivel, V.R., Kinjyo, I., Schambach, F., Intlekofer, A.M., Banerjee, A., Longworth, S.A., Vinup, K.E., Mrass, P., Oliaro, J., et al. (2007). Asymmetric T lymphocyte division in the initiation of adaptive immune responses. Science *315*, 1687–1691.

Du Pasquier, L. (2004). Innate immunity in early chordates and the appearance of adaptive immunity. C. R. Biol. *327*, 591–601.

Etienne-Manneville, S., Manneville, J.B., Nicholls, S., Ferenczi, M.A., and Hall, A. (2005). Cdc42 and Par6-PKCzeta regulate the spatially localized association of Dlg1 and APC to control cell polarization. J. Cell Biol. *170*, 895–901.

Fuchs, A., and Colonna, M. (2006). The role of NK cell recognition of nectin and nectin-like proteins in tumor immunosurveillance. Semin. Cancer Biol. *16*, 359–366.

Gajewski, T.F., and Fitch, F.W. (1988). Anti-proliferative effect of IFN-gamma in immune regulation. I. IFN-gamma inhibits the proliferation of Th2 but not Th1 murine helper T lymphocyte clones. J. Immunol. *140*, 4245–4252.

Galibert, L., Diemer, G.S., Liu, Z., Johnson, R.S., Smith, J.L., Walzer, T., Comeau, M.R., Rauch, C.T., Wolfson, M.F., Sorensen, R.A., et al. (2005). Nectin-like protein 2 defines a subset of T-cell zone dendritic cells and is a ligand for class-I-restricted T-cell-associated molecule. J. Biol. Chem. *280*, 21955–21964.

Geiger, B., Rosen, D., and Berke, G. (1982). Spatial relationships of microtubule-organizing centers and the contact area of cytotoxic T lymphocytes and target cells. J. Cell Biol. *95*, 137–143.

Holzer, U., Kwok, W.W., Nepom, G.T., and Buckner, J.H. (2003). Differential antigen sensitivity and costimulatory requirements in human Th1 and Th2 antigen-specific CD4+ cells with similar TCR avidity. J. Immunol. *170*, 1218–1223.

Hosken, N.A., Shibuya, K., Heath, A.W., Murphy, K.M., and O'Garra, A. (1995). The effect of antigen dose on CD4+ T helper cell phenotype development in a T cell receptor-alpha beta-transgenic model. J. Exp. Med. *182*, 1579–1584.

Humbert, P.O., Dow, L.E., and Russell, S.M. (2006). The Scribble and Par complexes in polarity and migration: friends or foes? Trends Cell Biol. *16*, 622–630.

Iezzi, G., Scotet, E., Scheidegger, D., and Lanzavecchia, A. (1999). The interplay between the duration of TCR and cytokine signaling determines T cell polarization. Eur. J. Immunol. *29*, 4092–4101.

Kennedy, J., Vicari, A.P., Saylor, V., Zurawski, S.M., Copeland, N.G., Gilbert, D.J., Jenkins, N.A., and Zlotnik, A. (2000). A molecular analysis of NKT cells: identification of a class-I restricted T cell-associated molecule (CRTAM). J. Leukoc. Biol. *67*, 725–734.

Krummel, M.F., and Macara, I. (2006). Maintenance and modulation of T cell polarity. Nat. Immunol. *7*, 1143–1149.

Kupfer, A., and Dennert, G. (1984). Reorientation of the microtubule-organizing center and the Golgi apparatus in cloned cytotoxic lymphocytes triggered by binding to lysable target cells. J. Immunol. *133*, 2762–2766.

Lee, G.R., Kim, S.T., Spilianakis, C.G., Fields, P.E., and Flavell, R.A. (2006). T helper cell differentiation: regulation by cis elements and epigenetics. Immunity *24*, 369–379.

Liang, S.C., Tan, X.Y., Luxenberg, D.P., Karim, R., Dunussi-Joannopoulos, K., Collins, M., and Fouser, L.A. (2006). Interleukin (IL)-22 and IL-17 are coexpressed by Th17 cells and cooperatively enhance expression of antimicrobial peptides. J. Exp. Med. *203*, 2271–2279.

Ludford-Menting, M.J., Oliaro, J., Sacirbegovic, F., Cheah, E.T., Pedersen, N., Thomas, S.J., Pasam, A., Iazzolino, R., Dow, L.E., Waterhouse, N.J., et al. (2005). A network of PDZ-containing proteins regulates T cell polarity and morphology during migration and immunological synapse formation. Immunity *22*, 737–748.

Ma, A., Koka, R., and Burkett, P. (2006). Diverse functions of IL-2, IL-15, and IL-7 in lymphoid homeostasis. Annu. Rev. Immunol. *24*, 657–679.

Maldonado, R.A., Irvine, D.J., Schreiber, R., and Glimcher, L.H. (2004). A role for the immunological synapse in lineage commitment of CD4 lymphocytes. Nature *431*, 527–532.

Mangan, P.R., Harrington, L.E., O'Quinn, D.B., Helms, W.S., Bullard, D.C., Elson, C.O., Hatton, R.D., Wahl, S.M., Schoeb, T.R., and Weaver, C.T. (2006). Transforming growth factor-beta induces development of the T(H)17 lineage. Nature *441*, 231–234.

Monks, C.R., Kupfer, H., Tamir, I., Barlow, A., and Kupfer, A. (1997). Selective modulation of protein kinase C-theta during T-cell activation. Nature *385*, 83–86.

Nagasaka, K., Nakagawa, S., Yano, T., Takizawa, S., Matsumoto, Y., Tsuruga, T., Nakagawa, K., Minaguchi, T., Oda, K., Hiraike-Wada, O., et al. (2006). Human homolog of Drosophila tumor suppressor Scribble negatively regulates cell-cycle progression from G1 to S phase by localizing at the basolateral membrane in epithelial cells. Cancer Sci. *97*, 1217–1225.

Osmani, N., Vitale, N., Borg, J.P., and Etienne-Manneville, S. (2006). Scrib controls Cdc42 localization and activity to promote cell polarization during astrocyte migration. Curr. Biol. *16*, 2395–2405.

Pear, W.S., Nolan, G.P., Scott, M.L., and Baltimore, D. (1993). Production of high-titer helper-free retroviruses by transient transfection. Proc. Natl. Acad. Sci. USA *90*, 8392–8396.

Round, J.L., Humphries, L.A., Tomassian, T., Mittelstadt, P., Zhang, M., and Miceli, M.C. (2007). Scaffold protein Dlgh1 coordinates alternative p38 kinase activation, directing T cell receptor signals toward NFAT but not NF-kappaB transcription factors. Nat. Immunol. *8*, 154–161.

Round, J.L., Tomassian, T., Zhang, M., Patel, V., Schoenberger, S.P., and Miceli, M.C. (2005). Dlgh1 coordinates actin polymerization, synaptic T cell receptor and lipid raft aggregation, and effector function in T cells. J. Exp. Med. *201*, 419–430.

Shingai, T., Ikeda, W., Kakunaga, S., Morimoto, K., Takekuni, K., Itoh, S., Satoh, K., Takeuchi, M., Imai, T., Monden, M., and Takai, Y. (2003). Implications of nectin-like molecule-2/IGSF4/RA175/SgIGSF/TSLC1/SynCAM1 in cell-cell adhesion and transmembrane protein localization in epithelial cells. J. Biol. Chem. *278*, 35421–35427.

Tanentzapf, G., and Tepass, U. (2003). Interactions between the crumbs, lethal giant larvae and bazooka pathways in epithelial polarization. Nat. Cell Biol. *5*, 46–52.

Teft, W.A., Kirchhof, M.G., and Madrenas, J. (2006). A molecular perspective of CTLA-4 function. Annu. Rev. Immunol. *24*, 65–97.

Trifari, S., Sitia, G., Aiuti, A., Scaramuzza, S., Marangoni, F., Guidotti, L.G., Martino, S., Saracco, P., Notarangelo, L.D., Roncarolo, M.G., and Dupre, L. (2006). Defective Th1 cytokine gene transcription in CD4+ and CD8+ T cells from Wiskott-Aldrich syndrome patients. J. Immunol. *177*, 7451–7461.

Xavier, R., Rabizadeh, S., Ishiguro, K., Andre, N., Ortiz, J.B., Wachtel, H., Morris, D.G., Lopez-Ilasaca, M., Shaw, A.C., Swat, W., and Seed, B. (2004). Discs large (Dlg1) complexes in lymphocyte activation. J. Cell Biol. *166*, 173–178.

Zeitler, J., Hsu, C.P., Dionne, H., and Bilder, D. (2004). Domains controlling cell polarity and proliferation in the Drosophila tumor suppressor Scribble. J. Cell Biol. *167*, 1137–1146.

Zheng, Y., Danilenko, D.M., Valdez, P., Kasman, I., Eastham-Anderson, J., Wu, J., and Ouyang, W. (2007). Interleukin-22, a T(H)17 cytokine, mediates IL-23-induced dermal inflammation and acanthosis. Nature *445*, 648–651.